

Microscopic probing of order-disorder versus displacive behavior in BaTiO₃ by Fe³⁺ EPR

K. A. Müller and W. Berlinger

IBM Zurich Research Laboratory, 8803 Rüschlikon, Switzerland

(Received 28 January 1986)

The cubic-crystalline field-splitting parameter a of Fe³⁺ at a Ti site in BaTiO₃ has been measured with EPR in the cubic phase as a function of pressure p and temperature T . From these measurements, the relative explicit volume and temperature dependences of $a(p, T)$ have been obtained. The former is *three* times those found in MgO, KTaO₃, or SrTiO₃. The relative explicit temperature dependence $(\partial \ln a / \partial T)_V$ is positive and *four and a half* times that found in inert MgO. In contrast, this effect is negative in KTaO₃ and SrTiO₃, where soft underdamped ferroelectric modes dominate. Both giant effects in BaTiO₃ point to a strong local Ti anharmonicity and ferroelectric order-disorder behavior in contrast to SrTiO₃ and KTaO₃.

I. INTRODUCTION

BaTiO₃ is the first ferroelectric oxide ever discovered.¹ The debate as to whether its transition is more displacive or order-disorder-like still continues.² Neutron and Raman scattering experiments clearly revealed a transverse-optical soft mode indicative of displacive behavior.^{3,4} However, the latter is highly overdamped near the cubic-tetragonal phase transition.³⁻⁵ Infrared-reflectivity experiments, including data in the tetragonal and orthorhombic phases, can be interpreted by strong relaxation excitations and a fading of the real part of the soft mode.^{6,7} Near-relaxation behavior is revealed in the 10¹¹–10¹²-Hz region by transmission experiments using backward-wave oscillators,⁸ allowing a reinterpretation of hyper-Raman data,⁵ as resulting from relaxator dynamics. All these new data indicate that, on cooling, one has to deal with a crossover phenomenon from displacive to order-disorder behavior.⁶ In the latter, large pretransitional correlated clusters, or rather chains, exist as revealed by the important and undisputed x-ray streaks in the cubic and ferroelectric phases.^{9,10} These intrinsic pretransitional correlations have been proposed¹¹ as being the cause of the anomalous temperature dependence of the index of refraction $n(T)$ in the cubic phase near T_c .¹² In an important paper, the anomalous part, $\Delta n(T)$, was pointed out as resulting from pretransitional fluctuations of the polarization $\langle \delta P^2 \rangle$.¹³

Whether a structural or ferroelectric transition is more displacive or order-disorder-like, i.e., whether an underdamped soft mode exists or relaxator dynamics are observed, depends on the local potential $V(\mathbf{R})$ of the ion or molecular unit in question. The displacive regime is characterized by a more harmonic $V(\mathbf{R})$ than the order-disorder one. In the simplest case, this can be approximated with the radial $R = |\mathbf{R}|$ dependence of $V(\mathbf{R})$ in single mode¹⁴ or statistical-mechanics^{15,16} theory as

$$V(R) = -AR^2 + BR^4, \tag{1}$$

with the constants A and B positive. Such a potential has minima at $R_m = \pm \sqrt{A/2B}$ with energy $V_m = (A/2)R_m^2$

(Fig. 1). The distinction between the limiting cases of displacive versus order-disorder¹⁶ behavior at the transition temperature T_c is determined by whether

$$V_m \ll kT_c \text{ (displacive) ,}$$

or (2)

$$V_m \gg kT_c \text{ (order-disorder) .}$$

From the above, it is important to obtain information on $V(\mathbf{R})$. For example, the cubic potentials of the Ti ion in SrTiO₃ and BaTiO₃ have to be different. In SrTiO₃, the ferroelectric (not structural) mode is *underdamped* but heavily *overdamped* in BaTiO₃.^{4,11} Therefore, one expects the Ti ion to move in quite a more harmonic potential in SrTiO₃ ($V_m < kT$) than in BaTiO₃ ($V_m > kT$). This is partly due to the larger size of the Ba²⁺ ion as compared to that of the Sr²⁺ one. The question, therefore, arises whether one can probe $V(\mathbf{R})$ microscopically. The next sections summarize EPR results on Fe³⁺ to this end, and show from three very large effects that BaTiO₃ is quite anharmonic and more of the order-disorder variety.

II. MICROSCOPIC EPR INFORMATION

Electron paramagnetic resonance is known to reflect the local environment of the paramagnetic ion, typically the position of the next neighbors in slightly covalent crystals. In a cubic environment, $V(\mathbf{R})$ can be written to

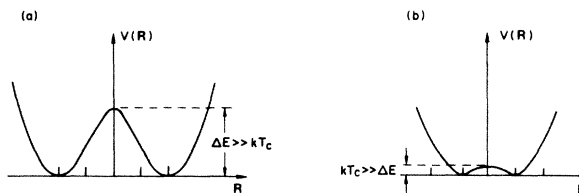


FIG. 1. Single-cell potentials in (a) order-disorder, (b) displacive structural-phase-transition systems. From K. A. Müller's introduction to Structural Phase Transitions (Ref. 16).

lowest order by

$$V(\mathbf{R}) = (x^4 + y^4 + z^4 - \frac{3}{5}R^4), \quad R^2 = x^2 + y^2 + z^2. \quad (3)$$

A paramagnetic singlet orbital ground state with spin $S \geq 2$ is split by (3) via spin-orbit and spin-spin interaction. The splitting is described empirically by a spin Hamiltonian of the form

$$\mathcal{H}_c = \frac{a}{6} [S_x^4 + S_y^4 + S_z^4 - \frac{1}{5}S(S+1)(3S^2 + 3S - 1)]. \quad (4)$$

For a Mn^{2+} or Fe^{3+} ion with half-filled $3d$ shell $3d^5$, $S = \frac{5}{2}$, the ${}^6S_{5/2}$ ground state is split into a Γ_8 quartet and a Γ_6 doublet by $3a$, which can be determined by EPR.¹⁷

The dependence of a on Fe^{3+} in various cubic oxides as a function of lattice spacing $2d$ was found to follow an empirical curve $a = a_0/d^n$ with $n \simeq 7$ and $\simeq 6$ near $d = 2$ Å, except for $SrTiO_3$, $BaTiO_3$, and $KNbO_3$.¹⁸ Whereas for $SrTiO_3$ the EPR parameter a is only slightly lower than the empirical curve, in the latter two crystals a is a factor of 2.5 smaller. Although this fact was pointed out a decade ago by Müller,¹⁸ it has not caught the attention of the ferroelectric community. Furthermore, the low a parameter correlates, as was then recognized, with the strongly overdamped and anisotropic soft modes in $BaTiO_3$ and $KNbO_3$ and the consecutive tetragonal, orthorhombic, and rhombohedral phases not observed in other perovskites. One of the reasons for the small amount of interest was the unclear theoretical relation of a to $V(\mathbf{R})$ for Fe^{3+} ; the position of this ion in the octahedral cell was not well understood, either.

An understanding of the position of Fe^{3+} in its octahedral cage was considerably improved with an analysis of Siegel and Müller.¹⁹ Using the superposition model to analyze some 20-year-old EPR second-order fine-structure splittings measured in the three ferroelectric phases of $BaTiO_3$ by Sakudo,^{20,21} it was shown that the Fe^{3+} remains centered in the octahedron. Thus, it is also clear why parameter a varies by no more than 10% in all phases of $BaTiO_3$.²¹ The reason why the Fe^{3+} remains centered is twofold. Fe^{3+} is nominally one unit negatively charged with respect to the Ti^{4+} it replaces, and therefore repels the negative nearest-neighbor O^{2-} ions, as follows from a recent theory of Sangster.²² Furthermore, the $3d$ shell of $Fe^{3+}(3d^5)$ is half-filled with the configuration $(t_{2g})^3(e_g)^2$. The e_g orbitals are antibonding and add repulsive forces between the Fe^{3+} and O^{2-} , whereas the t_{2g} are not antibonding. Cr^{3+} with configuration $(t_{2g})^3$ is still centered because of its negative effective charge but less than Fe^{3+} , owing to the two missing e_g electrons.²³ This behavior is nicely reflected in the recent tight-binding calculations of transition-metal ions in $SrTiO_3$ by Selme and Pecheur,²⁴ from which it follows that the t_{2g} orbitals are more localized on the oxygens surrounding the transition-metal ion, whereas the converse is true for the e_g orbitals. Furthermore, the too low charge of Fe^{3+} and Cr^{3+} pushed the t_{2g} levels up in the band gap of $SrTiO_3$ or $BaTiO_3$,^{24,25} whereas the ones of Mn^{4+} are close to the valence band.²⁴ The $Mn^{4+}(t_{2g})^3$ is isoelectronic to Cr^{3+} but the Sangster effect is absent: the Mn^{4+} charge is the same as the substitutional Ti^{4+} and its t_{2g} levels are delocalized by 65% on the oxygen atoms.²⁴ The Mn^{4+} thus

follows the cooperative motion of the Ti^{4+} and allows probing of Ti^{4+} dynamics.²⁶ Furthermore, its spin is $S = \frac{3}{2}$ and not split by (4). Therefore, the information gained by Fe^{3+} EPR via $a(d)$ is complementary to the one of Mn^{4+} .

To obtain information on $V(\mathbf{R})$, we can, with restrictions, take advantage of the empirical $a(d)$ dependence of Fe^{3+} in the following way. We first compute, from $a(d)$, how much larger d_{eff} in $BaTiO_3$ has to be than its actual lattice constant d to observe a reduced by a factor of 2.5 mentioned earlier. From the exponential law of a on d , we get $d_{eff}/d = (2.5)^{1/6} = 1.17$; i.e., the probing Fe^{3+} "sees" the oxygen atoms in $BaTiO_3$ at a 17% larger distance than what it should be for inert oxide. Now, we assume the minimum R_m of $V(|\mathbf{R}|)$ of (1) also at a distance larger by the same proportion, $R_m(BaTiO_3)/R(IO) = d_{eff}/d$, where IO stands for inert cubic oxide. Of course, $R_m \neq d$, but to lowest order their variation is proportional. With this, we calculate, for $V_m = (A/2)R_m^2$ in $BaTiO_3$, $V_m(BaTiO_3) = 1.34 V_m(IO)$, a 34% enhanced anharmonicity $\propto 1/B$. The same enhanced anharmonicity has also to be present in $KNbO_3$.

The question arises at this point whether additional experiments can confirm the conclusion reached above. This has indeed been the case most recently by measurements of the pressure p and temperature T dependences of the cubic-crystalline splitting parameter $a(p, T)$ described in Sec. III, whose total differential is given by

$$da = \left[\frac{\partial a}{\partial p} \right]_T dp + \left[\frac{\partial a}{\partial T} \right]_p dT. \quad (5)$$

$(\partial a / \partial p)_T$ and $(\partial a / \partial T)_p$ were first measured for Fe^{3+} and Mn^{2+} by Walsh,²⁷ then, using the differentiated form of the equation of state $V = V(p, T)$, where V is the volume, Walsh, Jeener, and Bloembergen²⁸ obtained the relation

$$\left[\frac{\partial a}{\partial T} \right]_p = -\frac{3\alpha}{\beta} \left[\frac{\partial a}{\partial p} \right]_T + \left[\frac{\partial a}{\partial T} \right]_V, \quad (6)$$

where $\alpha = (1/d)(\partial d / \partial T)_p$ is the coefficient of linear thermal expansion, and $\beta = -(3/d)(\partial d / \partial p)_T$, the volume compressibility. The first term on the right-hand side is the explicit volume effect, and the second, the explicit temperature effect. $(\partial a / \partial p)_T$ and $(\partial a / \partial T)_p$ were also measured earlier for Fe^{3+} in $SrTiO_3$ ²⁹ and more recently for $KTaO_3$.³⁰ In the latter publication, Rytz *et al.* compared the values obtained for Fe^{3+} and Mn^{2+} in MgO as well as Fe^{3+} in $SrTiO_3$ and $KTaO_3$. Two very interesting properties of $a(p, T)$ were noticed. The explicit volume effect relative to a was within 6% the same for all four measurements. The optic modes of either MgO , $SrTiO_3$, or $KTaO_3$, being underdamped, indicate quite harmonic potentials. The explicit temperature effect is negative in $KTaO_3$ and $SrTiO_3$, whereas it is positive for Mn^{2+} and Fe^{3+} in MgO . The negative contribution was attributed to the temperature dependence of the soft mode present in $SrTiO_3$ and $KTaO_3$, but absent in MgO .³⁰

The experiments on the pressure dependence in the cubic and tetragonal phases in $BaTiO_3$ are described in Sec. III, as well as the temperature dependence of a in the cubic phase. These are analyzed in Sec. IV with Eq. (6) and

yield *giant* relative explicit volume and temperature effects not found for any other oxide, three and over four times larger, respectively, and confirm also from their signs the enhanced anharmonicity in BaTiO₃ and its mainly relaxator-type dynamics.

III. EXPERIMENTAL PROCEDURE

A. Sample preparation

A BaTiO₃ single-crystal boule doped with 0.03 wt. % Fe₂O₃ has been grown by J. Albers with the top-seeded solution technique.^{23,31} After x-ray orientation along [100], two cylindrical samples with diameters of 0.7 and 0.9 mm were carefully shaped to lengths of 2.2 and 0.6 mm, respectively. The small sample size was imposed by the pronounced microwave damping at 19 GHz caused by this ferroelectric in the tetragonal phase. At ambient temperature, the Fe³⁺ signal was strong and the $|\pm\frac{3}{2}\rangle \rightarrow |\pm\frac{1}{2}\rangle$ fine-structure (FS) lines were roughly 30 G wide. This is about a factor of 3 narrower than the width observed in crystals from other sources,^{20,21} and is proof of the excellent quality of the BaTiO₃ used. Therefore, in the cubic phase, the $|\pm\frac{3}{2}\rangle \leftrightarrow |\pm\frac{1}{2}\rangle$ transitions were clearly resolved from the $|\pm\frac{5}{2}\rangle \leftrightarrow |\pm\frac{3}{2}\rangle$ lines.

For a magnetic field parallel to a $\langle 100 \rangle$ direction, the former fine-structure transitions with a Hamiltonian

$$\mathcal{H} = g\beta\mathbf{S} \cdot \mathbf{H} + \mathcal{H}_c \quad (7)$$

have a maximum splitting of $\Delta H = 5a/g\beta$ G. This quantity was measured as a function of temperature and pressure. It had earlier been reported above and below T_c .²⁰

B. Temperature dependence

The Fe³⁺ FS splitting in the cubic phase was measured in a water-cooled TE₀₁₁ cavity with a horizontally mount-

ed multistrip quartz heating element. Precise [100] crystal alignment was achieved by rotating the quartz-tube sample holder inside the heater, together with the magnet whose axis of rotation was perpendicular to the sample drive, until the FS splitting was at a maximum. For temperature control and reading, a 0.03-mm Pt–Pt–Rh thermocouple was placed on the sample. Thermal fluctuations never exceeded 10⁻² K up to the highest-temperature point measured at 640°C. Cavity design, temperature control, as well as their performances, have already been described in detail elsewhere.³²

Figure 2 shows the measured splittings of the $|\pm\frac{3}{2}\rangle \leftrightarrow |\pm\frac{1}{2}\rangle$ as a function of temperature from T_c at 135 to 640°C. The dependence is linear and its slope computed to be $\frac{1}{5}g\beta/hc(\Delta H/\Delta T)_p = -4.14 \times 10^{-4}$ cm⁻¹ K⁻¹. The constant $5a = 516$ G is $a = 96.6 \times 10^{-4}$ cm⁻¹ at T_c and is, within experimental accuracy, the one reported.²⁰ Table I compiles $(\partial a/\partial T)_p$ dependences including previous results in other cubic crystals such as MgO, SrTiO₃, and KTaO₃.

C. Pressure dependence

The hydrostatic EPR experiments were carried out in a sapphire-loaded TE₀₁₁ cavity similar to the one described by Wolbarst,³³ but scaled to 19 GHz. Silicon oil served as pressure-transmitting fluid, and a 1%-precision Bourdon gauge manometer monitored its pressure. Close to the cavity, a 100-Ω Pt resistor was imbedded in the beryllium-copper pressure bomb, and together with the afore-mentioned control system, the thermal variations were kept smaller than 3×10^{-2} K. To guarantee a reproducible position of the 0.7-mm-diam. sample in the presence of hydrostatic pressure, its (100) base was glued with epoxy onto a hollow brass holder. The magnetic field could be rotated in the (100) plane.

Figure 3(a) shows the increase in splitting of the outermost fine-structure lines $5a$ for $\mathbf{H}||[100]$ as a function of

TABLE I. The cubic-crystalline splitting parameter a of Fe³⁺ and Mn²⁺ and its measured temperature and pressure dependences.

	a (10 ⁻⁴ cm ⁻¹)	$\left[\frac{\partial a}{\partial T}\right]_p$ (10 ⁻⁶ cm ⁻¹ K ⁻¹)	$\left[\frac{\partial a}{\partial p}\right]_T$ (10 ⁻⁴ cm ⁻¹ kbar ⁻¹)
BaTiO ₃ :Fe ³⁺	97 ^a	-4.1 ^b	+2.52 ^b
KTaO ₃ :Fe ³⁺	305 ^c	-16.9 ^d	+2.55 ^e
SrTiO ₃ :Fe ³⁺	198 ^f	-11.0 ^g	+1.7 ^h
MgO:Fe ³⁺	205 ^h	-4.0 ⁱ	+0.9 ^j
MgO:Mn ²⁺	19.0 ^k	-0.51 ⁱ	+0.09 ^j

^aReference 20.

^bThis paper.

^cS. H. Wemple, Bull. Am. Phys. Soc. 8, 62, (1963).

^dReference 3.

^eReference 30.

^fK. A. Müller, Helv. Phys. Acta 31, 173 (1958).

^gReference 29.

^hW. Low, Proc. Phys. Soc. B 69, 1169 (1956).

ⁱReference 28.

^jReference 27.

^kW. Low, Phys. Rev. 101, 1827 (1956).

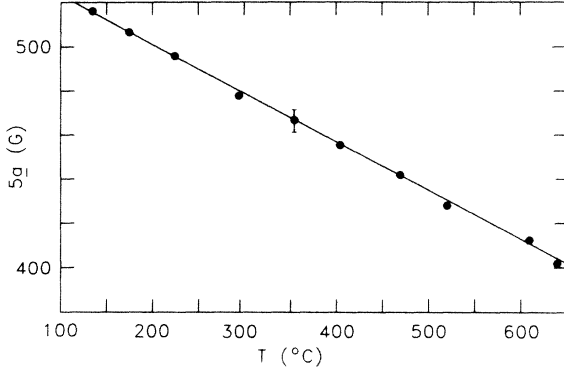


FIG. 2. Measured temperature dependence of the $|\pm\frac{3}{2}\rangle \rightarrow |\pm\frac{1}{2}\rangle$ cubic fine-structure splitting $5a$ for $\mathbf{H}||[100]$ in BaTiO_3 above T_c .

pressure at $T=134^\circ\text{C}$ just above T_c . A linear regression computation gave a slope of 13.0 G/kbar with a correlation coefficient $r=0.944$. This rather low coefficient was the reason for repeating the experiment at room temperature $T=24^\circ\text{C}$. At this temperature, the crystal is in the tetragonal ferroelectric phase. Therefore, an axial term in the Hamiltonian of the form

$$\mathcal{H}_{ax} = D[S_z^2 - \frac{1}{3}S(S+1)] \quad (8)$$

exists. This parameter varies as a function of pressure $(\partial D/\partial p)_T$ as well as the quantity of interest $(\partial a/\partial p)_T$. To obtain the latter, the splittings of the $|\pm\frac{3}{2}\rangle \leftrightarrow |\pm\frac{1}{2}\rangle$ and the one of the $|\pm\frac{5}{2}\rangle \leftrightarrow |\pm\frac{3}{2}\rangle$ lines were measured. The variation of all lines is shown in Fig. 4 for $\mathbf{H}||[100]$ as a function of p . The change of their splitting Δ from the total Hamiltonian

$$\mathcal{H}_T = g\beta\mathbf{S}\cdot\mathbf{H} + \mathcal{H}_c + \mathcal{H}_{ax}$$

is to lowest order

$$\begin{aligned} \Delta(\pm\frac{3}{2} \leftrightarrow \pm\frac{1}{2}) &= 4\Delta D - 5\Delta a, \\ \Delta(\pm\frac{5}{2} \leftrightarrow \pm\frac{3}{2}) &= 8\Delta D + 4\Delta a. \end{aligned} \quad (9)$$

The change in value of $5a$ computed with (9) from the

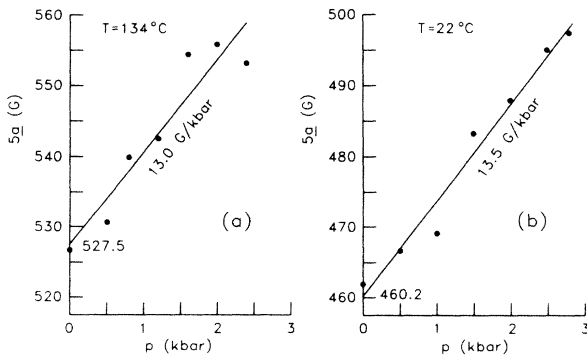


FIG. 3. Pressure dependence of the cubic fine-structure splitting $5a$ measured in (a) the cubic phase at $T_c=134^\circ\text{C}$; (b) evaluated in the tetragonal phase at room temperature from the data of Fig. 4 and Eq. (11).

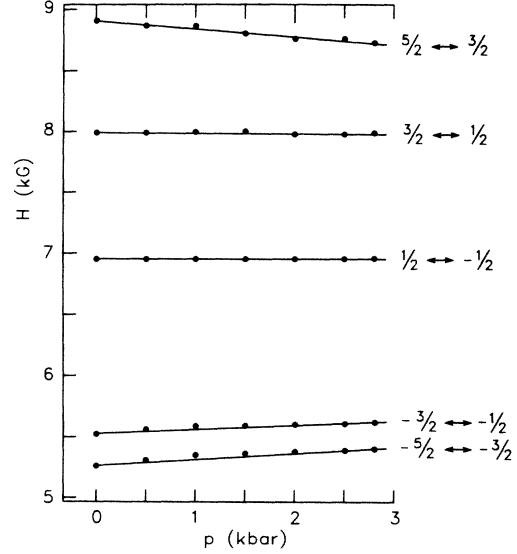


FIG. 4. Pressure dependence of all five fine-structure splittings of Fe^{3+} in BaTiO_3 at room temperature for a tetragonal domain parallel to $[100]||\mathbf{H}$.

data in Fig. 4 is plotted in Fig. 3(b). Their variation with pressure p is considerably more linear than those in Fig. 3(a). Indeed, the correlation coefficient in the linear regression $r=0.986$ closer to 1 indicates this. The slope obtained $(\partial 5a/\partial p)_T = 13.5$ G/kbar is essentially the same as that measured in the cubic phase. This is gratifying and proves that the cubic potential at the octahedral site measured from the center position, where the Fe^{3+} sits,¹⁹ shows the same anharmonicity. Converting this pressure coefficient into wave number per kbar, we get

$$\left[\frac{\partial a}{\partial p} \right]_T = \frac{g\beta}{5hc} \left[\frac{\partial a}{\partial p} \right]_T = 2.52 \times 10^{-4} \text{ cm}^{-1}/\text{kbar},$$

as listed in Table I, with the values determined in the other oxides. Although $(\partial a/\partial p)_T$ of BaTiO_3 is nearly the same as that found for KTaO_3 , we regard this as accidental because $(\partial a/\partial p)_p$ is 4.1 times that in BaTiO_3 . Actually, one has to compare the values obtained here for BaTiO_3 with all the others listed in Table I in a systematic way, as is done in the following section.

IV. ANALYSIS AND DISCUSSION

A. Evaluation of the explicit volume and temperature effect

EPR parameter a varies considerably from host to host and from the Fe^{3+} to the Mn^{2+} ion, as can be seen from the second column of Table I. Excluding BaTiO_3 for the moment, this is due to the d^{-6} dependence of a on the cubic host lattice constant $2d$ for a given ion (Fe^{3+}) and to the different spin-orbit constants between Fe^{3+} and Mn^{2+} . To obtain a meaningful comparison, one has, as outlined below, to look at the relative volume and therefore also the relative temperature dependences, i.e., the logarithmic derivatives of $a|(\partial \ln a/\partial x_i)_{x_j}$, where the x_i, x_j are the thermodynamic variables V, p , and T . From

Eq. (6), we have

$$\left[\frac{\partial \ln a}{\partial T} \right]_p = -\frac{3\alpha}{\beta} \left[\frac{\partial \ln a}{\partial p} \right]_T + \left[\frac{\partial \ln a}{\partial T} \right]_V. \quad (10)$$

The first term on the right-hand side is the relative explicit volume effect (REVE), and the second, the relative explicit temperature effect (RETE). The REVE was found to be essentially constant in the four cases investigated which were computed with the *bulk* linear thermal-expansion coefficients α and volume compressibilities β . They are $(3\alpha/\beta)(\partial \ln a/\partial p)_T = (3.6 \pm 0.2) \times 10^{-4} \text{ K}^{-1}$.³⁰ (See Note added in proof.) This constancy is the very reason for employing the logarithmic dependence, or better, one should say that it forces one to use it, as well as the bulk α and β coefficients. For the latter, this is the analog approach to using *bulk* lattice constants $2d$ to obtain $a(d)$.²⁰ One deals with pure empirical quantities, whereas the local relaxation, thermal expansion, and volume compressibility are not known; on the contrary, they are probed by these experiments.

In the cubic phase of BaTiO₃, α has not been measured systematically. There is one measurement at 160°C and one at T_c .³⁴ The slope between these two measurements is close to one computed from the linear thermal-expansion coefficients in the tetragonal phase $\alpha_a = \alpha_b = 15.7 \times 10^{-6} \text{ }^\circ\text{C}^{-1}$, $\alpha_c = 6.2 \times 10^{-6} \text{ }^\circ\text{C}^{-1}$, $\bar{\alpha} = \frac{1}{3}(\alpha_a + \alpha_b + \alpha_c) = 12.5 \times 10^{-6} \text{ }^\circ\text{C}^{-1}$.³⁵ The bulk compressibility is computed from the measured cubic elastic constants at 150°C, $S_{11} = 8.33 \times 10^{-12} \text{ m}^2/\text{N}$ and $S_{12} = -2.68 \times 10^{-12} \text{ m}^2/\text{N}$.³⁶ With the well-known formula $\beta = 3(S_{11} + 2S_{12}) = 8.91 \times 10^{-4} \text{ kbar}^{-1}$, we get

$$\frac{3\alpha}{\beta} = 4.21 \times 10^{-2} \text{ C}^{-1} \text{ kbar}^{-1}. \quad (11)$$

Using this value, the REVE and RETE are obtained with (11) and the measured quantities a , $(\partial a/\partial p)_T$, and $(\partial a/\partial T)_p$ are listed in Table I. They appear in the second column of Table II.

B. Comparison of results in BaTiO₃ with those in other cubic oxides

The relative explicit volume effect in BaTiO₃ $(3\alpha/\beta)(\partial \ln a/\partial p)_T$ is *three times* the average of $3.6 \times 10^{-4} \text{ K}^{-1}$ found in the other oxides! This is gigantic considering the 5% rms deviation for the other oxides. It is evidence that the local compressibility is much enhanced. This is actually what one expects from the 2.5-times-too-low absolute value of a in BaTiO₃ and KNbO₃: the too low a reflects the locally widening-up octahedral cage, as discussed in Sec. II, which becomes much more

compressed there than in a normal oxide. The REVE is so large that even if one assumed the absolute value of a to be normal in BaTiO₃, the REVE would overshoot the 5% rms value of other oxygens by 15%.

The second row in Table II compares the RETE found in BaTiO₃ with the values computed for the remaining oxides. Rytz *et al.*³⁰ have discussed the signs of the absolute effective temperature effect $(\partial a/\partial T)_V$. In the typical inert dielectric oxide MgO, it is positive, whereas it is negative in the incipient ferroelectrics SrTiO₃ and KTaO₃. It was pointed out in Ref. 30 that there are two contribu-

$$(\partial a/\partial T)_V \sim +f_1 - f_2 T_c / (T - T_c)^2, \quad (12)$$

a positive Debye contribution $+f_1$, and a negative soft-mode contribution $-f_2 T_c / (T - T_c)^2$. The RETE's listed in Table II show this in even clearer form than was the case in Ref. 30 for the absolute effective temperature effect. The values of Mn²⁺ and Fe³⁺ for MgO are almost the same. In this crystal, the soft-mode term is absent, whereas it is present in KTaO₃ and SrTiO₃. The two RETE values of KTaO₃ and SrTiO₃ are negative and comparable to one another. In contrast, the RETE is positive in BaTiO₃ and four and half times that in MgO! This giant positive RETE of $6.7 \times 10^{-4} \text{ K}^{-1}$ reflects substantial anharmonicity and therefore relaxator dynamics, masking a negative soft-mode contribution possibly present, which has to be of the order of $-2 \times 10^{-4} \text{ K}^{-1}$.

To visualize and compare our results, in Fig. 5(a) we plotted the scaled quantity $a(4.2/2d)^6$ as a function of $2d$, and in Figs. 5(b) and 5(c), the REVE and RETE from Table II. It should be noted that the ferroelectric PbTiO₃ with its underdamped soft mode lies close to the straight scaled line in Fig. 5(a), i.e., the Ti⁴⁺ ions "see" a quite harmonic potential and, as is well known, the Pb²⁺ is substantially involved in the soft mode. The arrows in Fig. 5 mark the deviation for BaTiO₃ from (a) the horizontal scaled line of a , (b) the average of the REVE in SrTiO₃, KTaO₃, MgO:Fe³⁺, and MgO:Mn²⁺, as well as (c) the distance from zero of the RETE. The arrows clearly indicate that in BaTiO₃ and KNbO₃, the local potential is more anharmonic compared to the other oxides, as quantitatively estimated in Sec. II.

Anharmonic dynamical lattice theory explains the soft mode and dielectric constants in the incipient ferroelectrics SrTiO₃, KTaO₃, and possibly in PbTiO₃; for example, in the work of Bruce and Cowley¹⁶ or in the more recent one of Migoni, Bilz, and Bäuerle.³⁷ However, the present findings put into question whether such a theory can quantitatively account for the classic three ferroelec-

TABLE II. Comparison of the relative explicit volume and temperature effects of Fe³⁺ in BaTiO₃ with those of Fe³⁺ and Mn²⁺ ions in cubic oxides. All numbers are in units of 10^{-4} K^{-1} .

Cubic oxide	BaTiO ₃ :Fe ³⁺	MgO:Fe ³⁺	MgO:Mn ²⁺	SrTiO ₃ :Fe ³⁺	KTaO ₃ :Fe ³⁺
$\frac{3\alpha}{\beta} \left[\frac{\partial \ln a}{\partial p} \right]_T$	+ 10.9	+ 3.4	+ 3.7	+ 3.8	+ 3.4
$\left[\frac{\partial \ln a}{\partial T} \right]_V$	+ 6.7	+ 1.46	+ 1.0	- 1.75	- 2.13

tric phase transitions in BaTiO_3 or KNbO_3 . Our Fe^{3+} EPR results point much more to Slater's original view of the "rattling Ti ion." Therefore, theories resulting from the electronic bands and densities appear at least as promising. In fact, from a vibronic approach, Bersuker³⁸ predicted a strong anharmonicity in BaTiO_3 with the minimum position of the Ti ion in all phases to lie along the $\langle 111 \rangle$ directions.

This prediction was verified independently with x-ray diffraction by Comes, Lambert, and Guinier.⁹ The controversy over whether these "static" observations could not also be explained by the dynamic anisotropic overdamped soft mode⁴ was recently solved by EPR of Mn^{4+} in BaTiO_3 .²⁶ This ion is magnetic, but in contrast to the Fe^{3+} , is sited near the Ti position. With this Mn^{4+} EPR study, a relaxational motion of the Ti^{4+} of the order of $\tau = 10^{-10}$ sec could be inferred, well below the range attainable by Raman,³ hyper-Raman,⁵ neutron scattering,⁴ or backward-wave oscillator¹⁸ techniques. The work presented here concurs with such a time τ because the EPR spectra of Fe^{3+} are observed in all phases of BaTiO_3 . This can only be the case if the reorientation time of the Ti ions in the high-temperature phases is much shorter than the time scale in the Fe^{3+} EPR experiment given by the crystalline splitting of $5a$, i.e., $(1/c)5a = 10^{-9}$ sec $\gg \tau \approx 10^{-10}$ sec.

V. CONCLUSION

The present pressure- and temperature-dependent experiments (in Sec. III) of the cubic ligand-field splitting parameter a of Fe^{3+} used as a microscopic probe in BaTiO_3 confirm the 34% enhanced anharmonicity of the Ti ion (see Sec. II), deduced from its absolute value as compared to other oxides. The relative explicit volume effect, REVE, $(3\alpha/\beta)(\partial \ln a / \partial p)_T$, is a factor of 3.0 larger as compared to the value of $(3.6 \pm 0.2) \times 10^{-4} \text{ K}^{-1}$ in the inert cubic oxide MgO as well as the incipient ferroelectrics SrTiO_3 and KTaO_3 . The constancy of the REVE in the latter cases proves that this is the quantity to compare the BaTiO_3 results with, and, through Eq. (10), also with the relative explicit temperature effect, RETE. The RETE $(\partial \ln a / \partial T)_V$ is positive, 4.5 times that in MgO, whereas it is negative in SrTiO_3 and KTaO_3 with underdamped soft modes. This confirms the substantial order-disorder character in BaTiO_3 (see Fig. 5). High-resolution x-ray-deduced Debye-Waller factor analyses by Ehses *et al.*³⁹ also point to a strong anharmonicity. Therefore, it is doubtful whether lattice dynamical theory^{16,37} is cap-

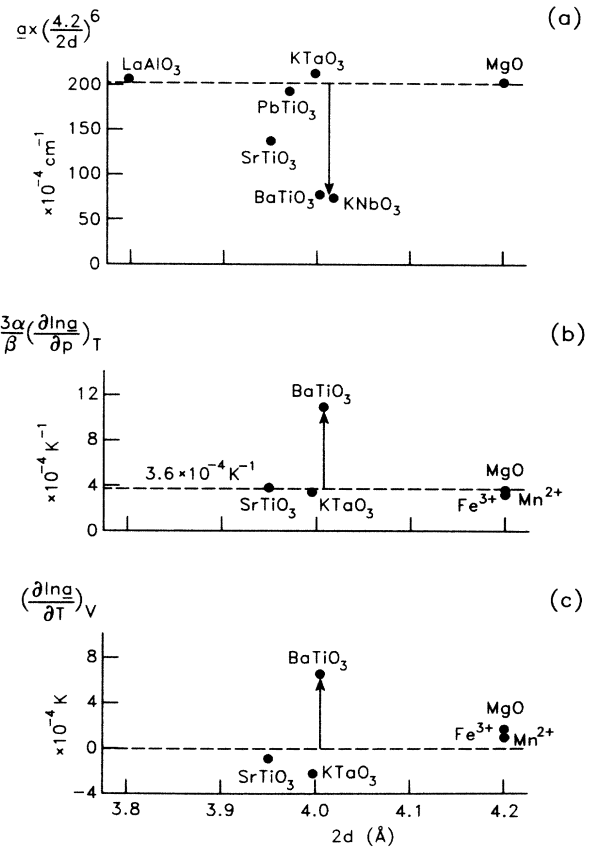


FIG. 5. Comparison of scaled cubic field-splitting parameter a , relative explicit volume and temperature effects in various cubic oxides as a function of lattice parameter $2d$.

able of dealing with this strong anharmonicity, and an approach starting with the adiabatic electronic structure is more realistic.³⁸ This is what most recent, in part *ab initio*, calculations attempt in a self-consistent way.^{40,41}

Note added in proof. For a given oxide, say MgO, $a = a_0 d^{-n_1}$, $n_1 = 21.2$.^{27,28} Therefore,

$$\frac{3\alpha}{\beta} \left[\frac{\partial \ln a}{\partial p} \right]_T = \alpha n_1 = 3.2 \times 10^{-4} \text{ K}^{-1},$$

close to the value of $3.4 \times 10^{-4} \text{ K}^{-1}$ experimentally deduced. However, from *one oxide to the other*,¹⁸ $n \approx 6 = n_1/3.5$ because of the different local oxygen relaxations occurring near the impurity.

¹M. E. Lines and A. M. Glass, *Principles and Applications of Ferroelectrics and Related Materials* (Clarendon, Oxford, 1977).

²Proceedings of the Sixth International Meeting on Ferroelectricity, Kobe, Japan, 1985, Symposium on Raman-, Submillimeter-, and Infrared-Spectroscopy (unpublished).

³P. A. Fleury and J. M. Worlock, *Phys. Rev.* **174**, 613 (1968).

⁴J. Harada, J. D. Axe, and G. Shirane, *Phys. Rev. B* **4**, 155 (1971).

⁵H. Vogt, J. A. Sanjurjo, and G. Rossbroich, *Phys. Rev. B* **26**,

5904 (1982).

⁶K. A. Müller, Y. Luspin, J. L. Servoin, and F. Gervais, *J. Phys. (Paris)* **43**, L-537, (1982).

⁷K. Inoue and N. Asai, *J. Phys. (Paris) Colloq.* **42**, C6-430 (1981).

⁸G. V. Kozlov, in Proceedings of the Sixth International Meeting on Ferroelectricity, Kobe, Japan, 1985 (unpublished).

⁹R. Comes, M. Lambert, and A. Guinier, *Solid State Commun.* **6**, 715 (1968).

¹⁰K. Itoh, L. Z. Zeng, E. Nakamura, and N. Mishima, *Fer-*

- roelectrics **63**, 29 (1985).
- ¹¹K. A. Müller, in *NATO 1981 School on Nonlinear Phenomena at Phase Transitions and Instabilities*, edited by T. Riste (Plenum, New York, 1982), p. 1; and *Statics and Dynamics of Nonlinear Systems*, Vol. 47 of *Solid-State Sciences*, edited by G. Benedek, H. Bilz, and R. Zeyher (Springer, Berlin, 1983), p. 68.
- ¹²G. Burns and F. H. Dacol, *Ferroelectrics* **37**, 661 (1981).
- ¹³R. Hofmann, S. H. Wemple, and H. Gränicher, *J. Phys. Soc. Jpn. Suppl.* **28**, 265 (1970).
- ¹⁴H. Thomas, in *Structural Phase Transitions and Soft Modes*, edited by E. J. Samuelsen, E. Andersen, and J. Feder (Universitetsforlaget, Oslo, 1971), p. 15.
- ¹⁵T. Schneider and E. Stoll, *Phys. Rev. Lett.* **31**, 1254 (1973); *Phys. Rev. B* **13**, 1216 (1976).
- ¹⁶More complete texts with the title "Structural Phase Transitions" are contained in two books: A. D. Bruce and R. A. Cowley, *Structural Phase Transitions* (Taylor and Francis, London, 1981); and *Structural Phase Transitions*, Vol. 23, of *Topics in Current Physics*, edited by K. A. Müller and H. Thomas (Springer-Verlag, Berlin, 1981).
- ¹⁷A. Abragam and B. Bleany, *Electron Paramagnetic Resonance of Transition Ions* (Clarendon, Oxford, 1970). For the latest results, see M. L. Du and M. G. Zhao, *J. Phys. C* **18**, 3241 (1985), and references therein.
- ¹⁸K. A. Müller, *Ferroelectrics* **13**, 381 (1976); *Phys. Rev. B* **13**, 3209 (1976).
- ¹⁹E. Siegel and K. A. Müller, *Phys. Rev. B* **19**, 109 (1979).
- ²⁰A. W. Hornig, R. C. Rempel, and H. E. Weaver, *J. Phys. Chem. Solids* **10**, 1 (1959).
- ²¹T. Sakudo, *J. Phys. Soc. Jpn.* **18**, 1626 (1963); and T. Sakudo and H. Unoki, *ibid.* **19**, 2109 (1964).
- ²²M. J. L. Sangster, *J. Phys. C* **14**, 2889 (1981).
- ²³K. A. Müller, W. Berlinger, and J. Albers, *Phys. Rev. B* **32**, 5837 (1985).
- ²⁴M. O. Selme, P. Pecheur, and G. Toussaint, *J. Phys. C* **17**, 5185 (1984); and M. O. Selme and P. Pecheur, *ibid.* **18**, 551 (1985).
- ²⁵F. M. Michel-Calendini and K. A. Müller, *Solid State Commun.* **40**, 255 (1981).
- ²⁶K. A. Müller, *Helv. Phys. Acta* **59**, 874 (1986).
- ²⁷W. M. Walsh, *Phys. Rev. Lett.* **4**, 507 (1960); *Phys. Rev.* **122**, 762 (1961).
- ²⁸W. M. Walsh, J. Jeener, and N. Bloembergen, *Phys. Rev.* **139**, A1338 (1965).
- ²⁹ $a(T)$ is linear in T , an apparent $\bar{a} = a_0 + 100/(T - 49)$ dependence reported by L. Rimai, T. Deutsch, and B. D. Silverman, *Phys. Rev.* **133** A1123 (1964), is due to the linewidth broadening approaching the structural 105-K phase transition. See also T. Revai, *Fiz. Tverd. Tela (Leningrad)* **10**, 3744 (1968) [*Sov. Phys.—Solid State* **10**, 2984 (1969)].
- ³⁰D. Rytz, U. T. Höchli, K. A. Müller, W. Berlinger, and L. A. Boatner, *J. Phys. C* **15**, 3371 (1982).
- ³¹J. Albers, First European Conference on Crystal Growth, Zurich, 1976 (unpublished), p. 150.
- ³²W. Berlinger, *Magn. Res. Rev.* **10**, 45 (1985).
- ³³A. B. Wolbrast, *Rev. Sci. Instrum.* **47**, 255 (1976).
- ³⁴H. F. Kay and P. Vousden, *Philos. Mag.* **40**, 1019 (1949).
- ³⁵R. G. Rhodes, *Acta Crystallogr.* **4**, 105 (1951).
- ³⁶D. Berlincourt and H. Jaffe, *Phys. Rev.* **111**, 143 (1958).
- ³⁷R. Migoni, H. Bilz, and D. Bäuerle, *Phys. Rev. Lett.* **37**, 1155 (1976).
- ³⁸I. B. Bersuker, *Phys. Lett.* **20**, 589 (1966); I. B. Bersuker, B. G. Vekhter, and A. M. Muzalevskii, *J. Phys. (Paris) Colloq., Suppl.* **4**, 33, C2-139 (1972), and references therein.
- ³⁹K. H. Ehses, H. Bock, and K. Fischer, *Ferroelectrics* **37**, 507 (1981).
- ⁴⁰L. Castet-Mejean and F. M. Michel-Calendini, *Ferroelectrics* **37**, 503 (1981).
- ⁴¹K. H. Weyrich and R. Siems, *Z. Phys. B* **61**, 63 (1985).